Contributed paper

OPTO-ELECTRONICS REVIEW 9(1), 67–74 (2001)

Epitaxial RE^{3+}:YAG planar waveguide lasers

M. MALINOWSKI*[1], J. SARNECKI[2], R. PIRAMIDOWICZ[1], P. SZCZEPAŃSKI[1], and W. WOLIŃSKI[1]

[1]Institute of Microelectronics and Optoelectronics Warsaw, University of Technology
75 Koszykowa Str., 00-662 Warsaw, Poland
[2]Institute of Electronic Materials Technology 133 Wólczyńska Str., 01-919 Warsaw, Poland

The interest in increasing signal speed, lowering optical losses and reducing power requirements led to the integration and miniaturisation of the optoelectronics components. Planar optical devices play an increasingly important role as the components for fibreoptic communication and optical computing systems. Their purpose is to couple, switch, modulate, amplify or generate optical signal. Recent important development is successful operation of planar waveguide amplifiers and lasers that could be easily coupled to fibre components. Several waveguide fabrication techniques are employed depending on host material, including semiconductor materials, dielectric crystals and glasses.

In this work the basic problems related to active waveguide fabrication and properties will be discussed. We also report the spectroscopic and laser properties of the Nd^{3+}:YAG/YAG epitaxial thin films obtained in ITME laboratory in Warsaw.

Keywords: waveguide lasers, thin films, YAG, rare-earth ions, LPE.

1. Introduction

Planar optical devices play increasingly important role as the components for fibreoptic communication systems. By using optical fibres for data transfer, transmission rates of the order of 10 Gbit/s and bandwidths of several nm could be achieved [1,2]. The interest in increasing signal speed, lowering optical losses and reducing power requirements led to integration and miniaturisation of the optoelectronic components. Their purpose is to couple, switch, modulate, amplify or generate optical signal. Recent important development is successful operation of planar waveguide amplifiers and lasers that could be easily coupled to fibre components [3,4]. Several waveguide fabrication techniques are employed depending on host material, including semiconductor materials, dielectric crystals and glasses [5]. It was recently proved that planar lightwave circuits based on silica waveguides offer an attractive and low-cost technology for both passive and active devices [6–8].

At present, most of the optical telecommunication through optical fibres takes place at the wavelengths of 1.5 μm (coinciding with the transmission maximum of standard silica fibre) and 1.3 μm (coinciding with the high transmission and dispersion minimum of silica fibre). Thus, trivalent erbium (Er^{3+}) doped materials which show optical emission at 1.54 μm [9] and praseodymium (Pr^{3+}) doped materials for the 1.3 μm range, which both could be pumped by IR diode lasers, are extensively studied.

1.3-μm emission of the praseodymium ion is due to transition from the excited $^1G_4$ state to the $^3H_5$ multiplet and from the energy level diagram of Pr^{3+} it results that optimum pumping wavelength is around 1.02 μm [10]. A solid state laser is an alternative praseodymium-doped fibre amplifier (PDFA) pump source because it has the high output power and frequency stability. One of the candidates for PDFA pump is a 968-nm laser diode (LD) pumped 1.03 μm Yb:YAG laser. However, because of the high costs of this LD, Yb+Nd:YAG waveguide laser pumped at 810 nm and operating at 1.03 μm, as a result of efficient energy transfer from Nd to Yb ions, has been proposed [11]. Because of the short optical lengths, high absorption and high gains are needed for waveguide lasers. Thus, materials with high concentration of active ions should be used. In the 70's, several papers on waveguide lasers fabricated from the stoichiometric neodymium (Nd^{3+}) compounds (phosphates and borates) have been published [12–15].

The basic problems related to active waveguide fabrication and properties will be discussed in this work. We also report spectroscopic and laser properties of the Nd^{3+}:YAG/YAG epitaxial thin films and waveguide structures obtained by means of liquid phase epitaxy in ITME laboratory in Warsaw.

*e-mail: malinowski@imio.pw.edu.pl

2. Principles of operation of waveguide planar devices

The simples optical planar waveguide consists of a planar film of refractive index n_f surrounded by the substrate and cover layers with lower refractive indices n_s and n_c respectively (Fig. 1). The light is confined in the n_f layer by total internal reflections at the layers interfaces. This requires that $n_f > n_s > n_c$ and typical differences in refractive indices range from 10^{-3} to 10^{-1}. By solving the Maxwell's equations in one dimension system [16-18] under boundary conditions at surfaces and assuming **E** and **H** fields with a periodic time dependence of the form

$$\boldsymbol{E}(t) = \boldsymbol{E}(x,y,z)\exp(i\omega t) + \boldsymbol{E}^*(x,y,z)\exp(-j\omega t), \quad (1)$$

where **E** is the complex amplitude, ω is the angular frequency, we arrive at wave equations for field solutions of the form

$$\boldsymbol{E}(x,y,z) = \boldsymbol{E}_q(x,y)\exp(-j\beta_q z), \quad (2)$$

and

$$\boldsymbol{H}(x,y,z) = \boldsymbol{H}_q(x,y)\exp(-j\beta_q z), \quad (3)$$

where q is a mode number and β_q is the propagation constant of the mode. A planar guide supports transverse electric (TE) modes with zero longitudinal electric field ($E_z = 0$) and transverse magnetic modes (TM) with zero magnetic field ($H_z = 0$). The wave equations governing TE and TM modes are

TE:
$$\frac{\partial^2 E_y}{\partial x^2} = (\beta^2 - n^2 k^2)E_y, \quad (4)$$

where

$$k = \omega/c = \omega(\varepsilon_o m_o)^{1/2} \quad (5)$$

and

TM:
$$n^2 \frac{\partial}{\partial x}\left(\frac{1}{n^2}\frac{\partial H_y}{\partial x}\right) = (\beta^2 - n^2 k^2)H_y. \quad (6)$$

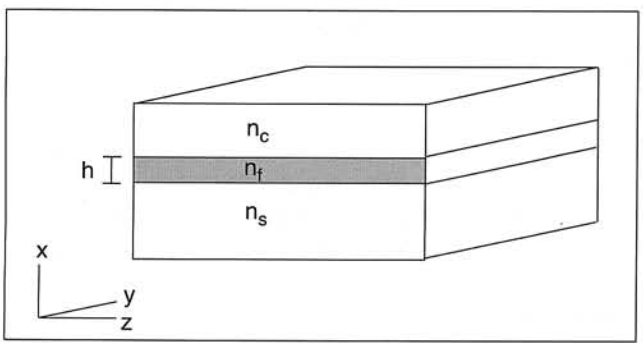

Fig. 1. Scheme of planar dielectric waveguide.

The boundary conditions demand that E_y (and thereby H_x and H_z) be continuous across the film boundaries at x = 0 and x = h. Thus, the field E_y distribution in the three considered regions are

$$E_y = E_c \exp[-\gamma(x-h)], \quad \text{for } h < x, \quad \text{(cover)}$$
$$E_y = E_f \cos[\gamma_f x - \phi_s)], \quad \text{for } 0 < x < h, \quad \text{(film)} \quad (7)$$
$$E_y = E_s \exp[\gamma_s x], \quad \text{for } x < 0, \quad \text{(substrate)}$$

where γ_i (i = c, f, s) are the propagation constants defined by

$$-\gamma_i^2 = n_i^2 k^2 - \beta^2. \quad (8)$$

Application of the boundary conditions gives the eigenvalue equation for the propagation constant b, known also as the dispersion relation of the form

$$h\sqrt{n_f^2 k^2 - \beta^2} - \Phi_s - \Phi_c = m\pi, \quad (9)$$

where m is the mode order, and the phase shifts Φ_s and Φ_c for the total reflections at the waveguides boundary are given by

$$\Phi_i = \arctan q_i \frac{\gamma_i}{\gamma_f}, \quad (10)$$

$$q_i = \left.\begin{matrix} 1 \\ n_f^2/n_i^2 \end{matrix}\right\} \text{ for } \begin{matrix} \text{TE} \\ \text{TM} \end{matrix} \text{ modes} \quad (11)$$

Example of the dependence of "h" on the effective refractive index $n_{eff} = b/k$ of the guided modes is presented in Fig. 2. It could be seen that for a given h there is a discrete spectrum of b values and that n_{eff} value lies between n_s and n_f. As the guide gets thicker it allows more guided modes to propagate, for a very thin film it results that the guide cannot always support a guided mode and there is a cut-off thickness for a fundamental mode. We can define cut-off waveguide thickness for mode m h_m in terms of the refractive index values

$$h_m = \frac{1}{k_o\sqrt{n_f^2 - n_s^2}}\left(arctg\sqrt{\frac{n_s^2 - n_c^2}{n_f^2 - n_s^2}} + m\pi\right). \quad (12)$$

It results from Eq. (12) that waveguide mode selection could be realised by influencing layer thickness and ($n_f - n_s$) index difference. Waveguide is single mode for the normalised thickness lying between 0 and P. Thus optimum effective thickness for the symmetric guide is given by

$$h_{opt} = 0.780\frac{\lambda}{\sqrt{n_f^2 - n_s^2}}. \quad (13)$$

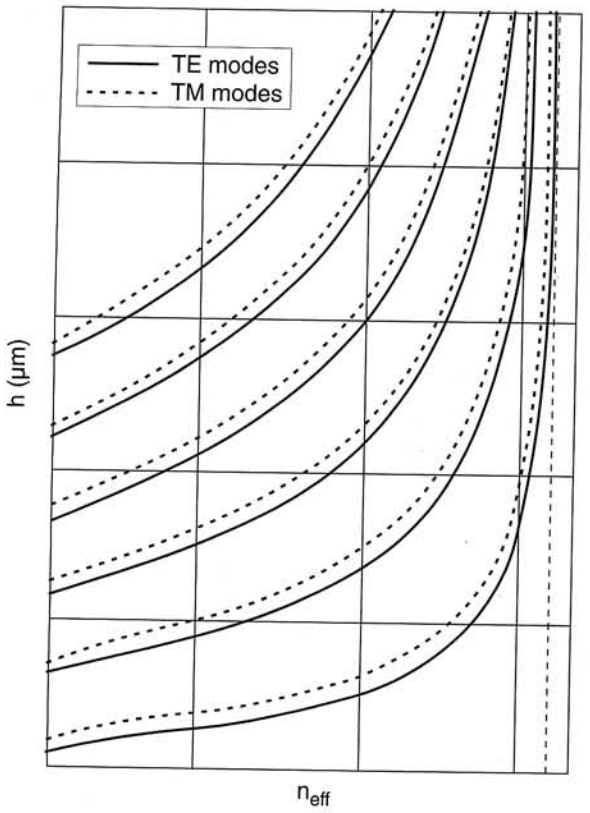

Fig. 2. Dependence of the film thickness "h" on the effective refractive index n_{eff}.

In Fig. 3, h_{opt} is presented as a function of $(n_f - n_s)$ for the wavelength of 1.06 μm. It could be seen that the index difference of about 10^{-2} is necessary for single mode operation of a film of about 5 μm thickness.

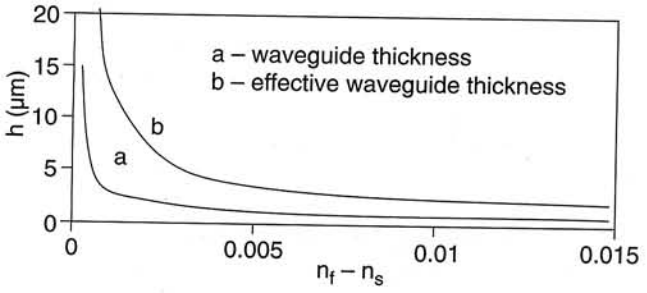

Fig. 3. Optimum effective waveguide thickness vs. refractive index.

3. Fabrication of planar lasers and amplifiers

Planar active optical waveguides are fabricated by a variety of techniques in numerous hosts including semiconductor materials, dielectric crystals and glasses. Depending on the type of substrate being used and the intended application such techniques as diffusion, liquid phase epitaxy (LPE), molecular beam epitaxy (MBE), implantation, physical vapour deposition and ionic exchange have been reported to generate optical waveguides.

Ion implantation is a widely used technique for doping waveguides with optically active ions. It offers excellent control over the position and dose of the introduced dopants and Er implanted silica planar structures have been demonstrated [6]. High-energy (up to 3 MeV) He^+ implantation, can be used to alter controllably refractive index profile allowing formation of optical waveguides in a wide range of substrate materials.

To the date ion implantation has been the principal technique for fabrication of planar active optical structures within laser gain media such as Er:YAG, Nd:YAG, or Yb:YAG [21–24]. Because of the important structural damage of the material the optical losses of this kind of waveguides are of the order of 1 dB/cm, damage can also couple to the active ion, and thereby case non-radiative decay which lowers the luminescence quantum efficiency.

Liquid phase epitaxy (LPE) is a promising technique for producing low-loss (<0.05 dB/cm) planar wavequide lasers. In particular, rare earth doped YAG epitaxial layers on YAG substrate have been demonstrated to have excellent laser properties. Due to gallium (Ga) substitution in the active layer the refractive index differences $(n_f - n_c)$ up to 5×10^{-2} could be produced. The introduction of a large concentration of gallium requires the lattice mismatch compensation with lutetium (Lu). Lattice mismatch versus dopant concentration and film-substrate refractive index difference versus Ga concentration are presented, after Refs. 19 and 20 in Figs. 4 and 5.

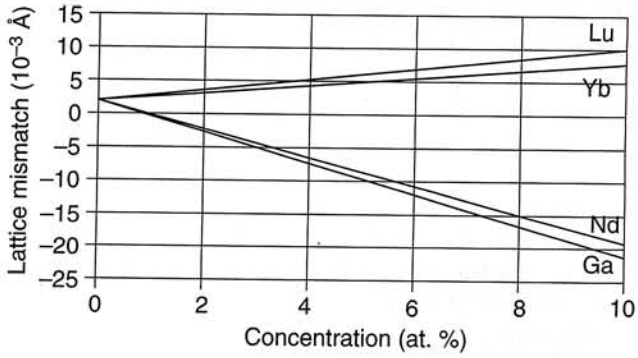

Fig. 4. Lattice mismatch difference vs. dopant concentration in film (after Refs. 19 and 20).

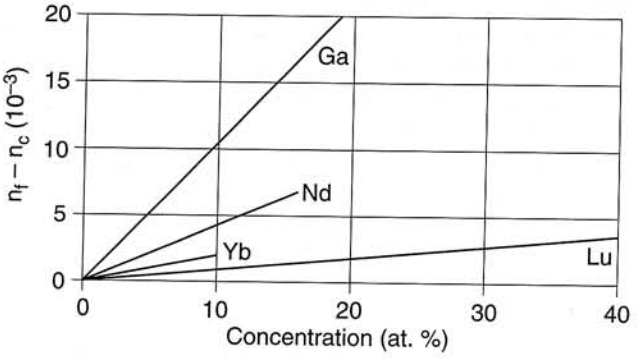

Fig. 5. Film substrate refractive index difference vs. dopant concentration (after Refs. 19 and 20).

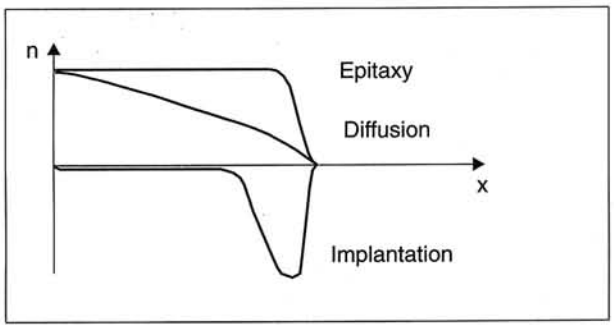

Fig. 6. Refractive index profiles for different waveguide technologies.

The refractive index profiles depend on the method of waveguide preparation (see Fig. 6). Diffusion technique generally results in smooth variation of the refractive index. Liquid phase epitaxy of higher index material on the substrate surface gives step index changes. Proton implantation, in most materials, results in decrease in the refractive index that forms an optical barrier at the depth corresponding to the penetration distance of the high-energy He^+ ions.

4. Liquid phase epitaxy of waveguides and lasers

The first successful laser experiments in epitaxial Ho^{3+}:YAG layers on YAG substrates were reported by Van der Ziel *et al.* [25] in 1972 and the reports on laser oscillations from Ho^{3+} and Nd^{3+} ions in LPE grown YAG thin films were presented in 1973 [26]. More detailed experimental studies of laser Nd^{3+}:YAG/YAG structures, including DFB and DBR resonators, were presented in Ref. 18. Because of relatively high losses, of the order of 1 dB/cm, resulting from the high dislocation density and incorporation of lead impurities in the epitaxial layers, thresholds were high and efficiencies were low allowing generation under intense pumping by flashlamps or cw argon laser. With the improvement in the LPE process [20,26,27], miniaturised diode-pumped waveguide lasers with submilliwatt thresholds were obtained [19,28].

Recently, much interest has been focused on Yb^{3+} -doped solid-state lasers. A 1.03-μm Yb^{3+}:YAG laser has the output wavelength close to the absorption centre of Pr^{3+} doped fibre and is a good candidate for PDFA pump source [11]. Efficient, diode-pumped room temperature, bulk Yb^{3+}:YAG laser has been presented by Lacovara *et al.* [29] in 1991. Recently, Pelenc *et al.* reported the 1.03-μm and 1.05-μm laser operation of a diode-pumped Yb^{3+} doped YAG planar waveguide [19]. Ytterbium activated YAG films were grown by means of LPE technique and estimated optical losses at the laser wavelength were less than 0.1 dB/cm. The resonator consisted of two plane parallel mirrors with the 2.3% output transmission at 1.03 μm. An InGaAs 1-W diode laser emitting around 968 nm was used as the pump [19]. Very high slope efficiency, of about 77% and low thresholds of about 43 mW were registered, which are better than observed in a bulk Yb^{3+}:YAG systems.

A room-temperature operation of an Yb-doped $Gd_3Ga_5O_{12}$ buried channel waveguide laser at 1.025 μm wavelength has been reported [30]. The buried channel waveguide was prepared on an Yb^{3+}:GGG film grown on a GGG substrate by means of LPE. A Ti:Al_2O_3 laser was used as the pumping light source and the observed threshold and slope efficiency were 80 mW and 13.6% respectively. The authors concluded that the parameters of this device could be increased after coupling losses optimisation.

5. LPE growth of Nd:YAG/YAG waveguide structures

Recently, in ITME laboratory in Warsaw, the layers of Nd:YAG/YAG have been grown from a supercooled (supersaturated) molten garnet-flux high temperature solution. Standard isothermal LPE dipping technique with reversed axial rotation has been used to YAG thin film doped with Nd^{3+}, Ga^{3+} and Lu^{3+} ions.

The supersaturation ΔT which is the saturation (liquidus) temperature T_S minus the growth temperature T_G is necessary for epitaxial growth of garnet layer from garnet – flux (PbO-B_2O_3) solution.

The epitaxy equipment used for LPE growth of garnet thin layers was constructed in the Institute of Electronic Materials Technology in Warsaw in co-operation with the Industrial Institute of Automation and Measurements in Warsaw. The LPE dipping equipment consists of resistant heated three-zone furnace, rotation and translation microprocessor control module cooperated with three sets of Eurotherm temperature controller of 815P type. The accuracy of temperature control is ±1.0°C so, it is possible to form the vertical temperature gradient in the melt of about 0.5°C/cm. Evaporating PbO was exhausted.

Garnet layers were grown on <111> oriented 20-mm diameter YAG substrates using the isothermal dipping technique with rotation of the horizontally held substrate in Pt holder. The procedure of melt preparation and the dipping process was identical that the developed for magnetic bubble garnet and has been reported in many papers [31,32].

The composition of molten garnet-PbO-B_2O_3 high temperature solution are specified by the following parameters

$$R_1 = \frac{[Al_2O_3]}{[Y_2O_3 + Nd_2O_3 + Lu_2O_3]} \qquad R_2 = \frac{[Al_2O_3]}{[Ga_2O_3]} \qquad R_3 = \frac{[PbO]}{[B_2O_3]}$$

$$R_4 = \frac{[Y_2O_3 + Nd_2O_3 + Lu_2O_3 + Al_2O_3 + Ga_2O_3]}{[Y_2O_3 + Nd_2O_3 + Lu_2O_3 + Al_2O_3 + Ga_2O_3 + PbO + B_2O_3]} \qquad R_5 = \frac{[Y_2O_3]}{[Nd_2O_3 + Lu_2O_3]}$$

These are the same molar compositional ratios of the melt elements introduced by Blank *et al.* for the epitaxy of magnetic garnets [32]. R_i parameters are important in determining the growth conditions and properties of the films.

The compositions of garnet thin layers could be expressed by the following formula: $Y_{3-x-y}Nd_xLu_yAl_{5-z}Ga_zO_{12}$, where x, y and z are the Nd, Lu concentrations in dodecahedral sites and z is the Ga concentration in tetrahedral sites, respectively.

At first, Nd:YAG films with neodymium concentration of around 1 at.% and luminescence lifetime of 260 μs were grown from the melt No. 1. Then, substitutions with neodymium, gallium and lutetium were carried out. The good quality films with the thickness up to 30 μm were prepared at supercooling of about 15°C.

R_i parameters for the growth of $Y_{3-x-y}Nd_xLu_yAl_{5-z}Ga_zO_{12}$ (Nd^{3+} ions concentration is constant – about 1 at.%, x = 0.03) with different concentration of Ga^{3+} and Lu^{3+} ions, the growth temperature T_G, and estimated from X-ray diffraction measurements compositional parameters y and z in the formula of garnet layers composition are listed in Table 1 [33].

Table 1. R_i composition parameters and the concentrations of Lu^{3+} and Ga^{3+} ions in YAG epitaxial films and waveguides.

No.	R_1	R_2	R_3	R_4	R_5	T_s (°C)	y	z
1	5.0	–	12.0	0.0294	14.0	1048	–	–
2	5.0	11.55	12.02	0.0295	13.99	1041	0	~0.07
3	5.0	5.775	12.02	0.030	13.99	1032	0	~0.25
4	4.74	2.8875	12.02	0.0317	7.82	1021	0.3	≥0.4
5	4.52	2.8875	12.02	0.0319	5.42	1015	0.5	≥0.4
6	5.0	12.0	12.0	0.029	13.9	1018	0	~0.09
7	5.0	6.0	12.0	0.030	13.9	1015	0	~0.26
8	4.46	2.887	12.0	0.0321	4.98	1015	0.6	~ 0.7
9	4.14	2.887	12.0	0.0324	3.41	1013	0.9	~0.7

6. Characterisation of the Nd:YAG/YAG waveguide structures

The differences between films and substrate lattice constants were measured by X-ray high-resolution diffraction [33,34].

For epitaxial structures grown from melt No 9, X-ray rocking curve presented in Fig. 7 indicates no peak separation. It means that the lattice constants of the epitaxial film and the substrate are practically equal and we have obtained the best lattice mach for our waveguide structures.

The refractive index of the layer has been measured using Pluta's double-refracting interference microscope in its transmitted-light version. The results of the refractive index difference Δn measurements were shown in our earlier paper [33]. In gallium and lutetium substituted garnet wave-

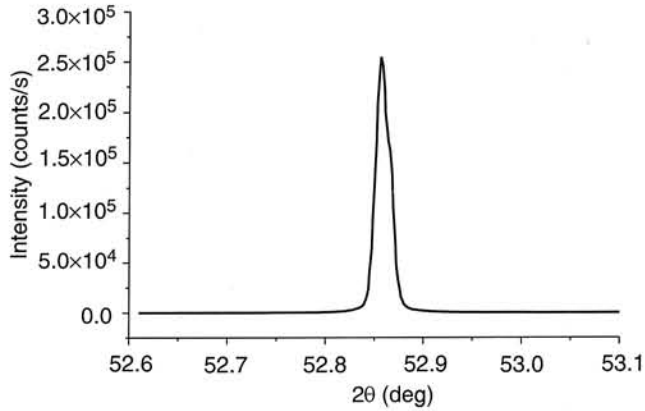

Fig. 7. XRD pattern of $Y_{3-x-y}Nd_xLu_yAl_{5-z}Ga_zO_{12}$/YAG epitaxial structure (melt No 9).

guide layers $Y_{3-x-y}Nd_xLu_yAl_{5-z}Ga_zO_{12}$, with concentration of Nd^{3+}, Lu^{3+} and Ga^{3+} ions of about 1 at.% (x = 0.03), 30 at.% (y = 0.9) and 14 at.% (z = 0.7), we have obtained Δn up to 2×10^{-2} at a wavelength λ of 0.6328 μm, respectively.

Absorption spectrum in the diode laser pumping band is shown in Fig. 8. After excitation at 808 nm emission spectra of Nd^{3+}:YAG/YAG structure as a function of active ion concentration have been registered in the 1.06 μm band and they are presented in Fig. 9. After pulsed laser excitation measurements of the $^4F_{3/2}$ fluorescence lifetime have been performed for different neodymium ion concentration. The results of these measurements are shown in Fig. 10. It could be observed that lifetimes and decay transients are strongly concentration dependent reflecting the quenching effect due to cross-relaxation between two neighbouring neodymium ions [33]. Comparison of the measured lifetimes with the literature data is presented in Table 2.

Next, optical amplification and laser generation at 1.06 μm has been investigated in the experimental set-up shown schematically in Figs. 11 and 12. The planar waveguide samples typically of 5×10 mm were cut from epitaxial structures. The surfaces of end faces were polished to high laser quality to allow longitudinal-pumping

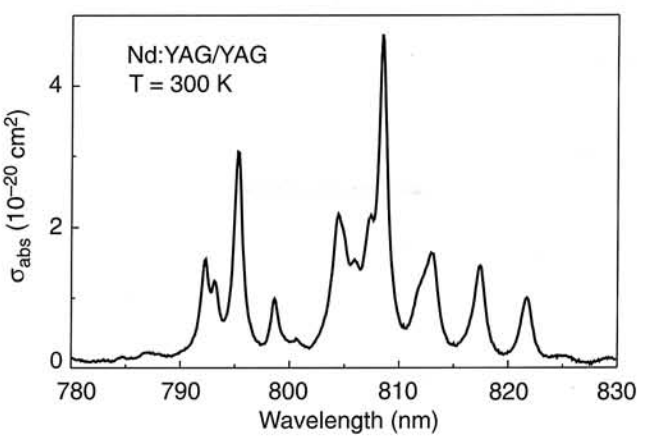

Fig. 8. Absorption cross-section spectrum in the diode laser pumping band.

Table 2. Fluorescence lifetims vs. neodymium ion concentration.

Material	$Y_3Al_5O_{12}$:1% Nd^{3+}	$Y_3Al_5O_{12}$:3% Nd^{3+}	$Y_3Al_5O_{12}$:6% Nd^{3+}
τ_{lum} (μs) – crystal	255	200 (flux growth)	75 (flux growth)
τ_{lum} (μs) – waveguide	267	~220	~77

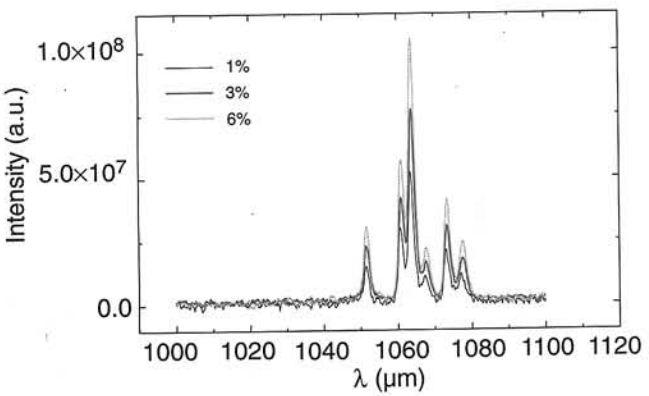

Fig. 9. 1.06-μm emission spectrum of Nd:YAG films vs. Nd^{3+} concentration.

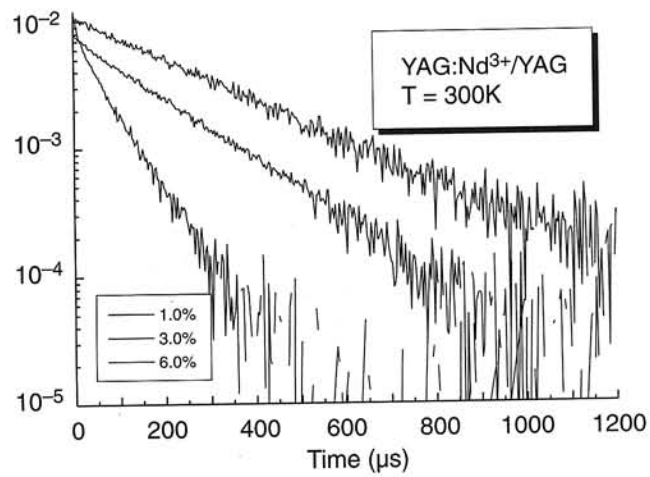

Fig. 10. Decay profiles of $^4F_{3/2} \rightarrow {}^4I_{9/2}$ luminescenc in Nd:YAG films.

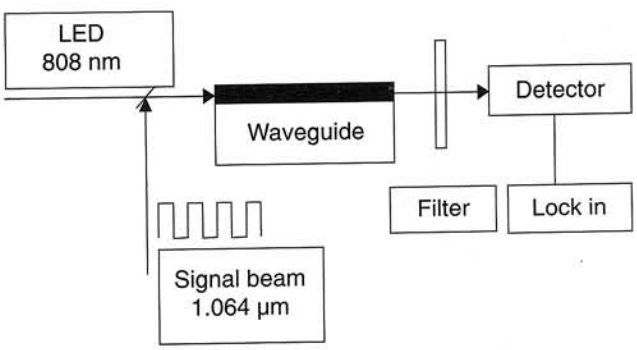

Fig. 11. Schematic diagram of the experimental setup for small signal gain measurement.

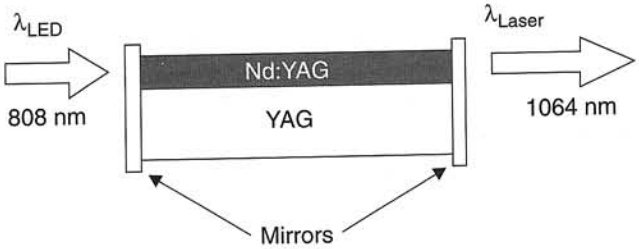

Fig. 12. Planar waveguide Nd:YAG laser.

structures. The signal beam at 1.064 μm, corresponding to the maximum of the YAG:Nd^{3+} emission, and the pumping beam at 808 nm were injected simultaneously to the waveguide. Signal beam has been mechanically modulated and registered after passing through the waveguide as a function of pumping power. Small signal gain of 18 dB has been observed at 1.064 μm.

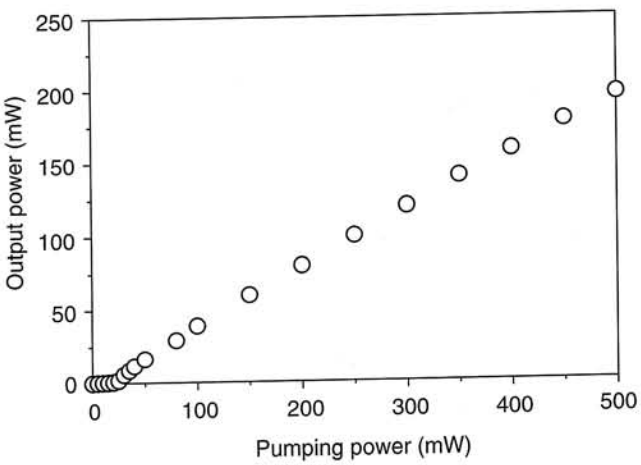

Fig. 13. Output power vs. incident pump power for the $Y_{3-x-y}Nd_xLu_yAl_{5-z}Ga_zO_{12}$ waveguide laser.

Laser experiments have been performed in the plane-parallel Fabry-Perot resonator. The mirrors of 0 and 5% transmission at 1.064 μm have been placed directly at the waveguides surfaces. Lasing has been observed at the threshold pumping power of about 25 mW (Fig. 13), which allows estimating the distributed loss coefficient to be less than 0.1 dB/cm.

7. Conclusions

As indicated by X-ray diffraction, refractive index data, optical spectroscopic studies, amplification and laser measurements good optical quality and high cristallinity epi-

taxial films and waveguide structures have been grown in ITME on YAG substrates opening perspectives for miniature, high efficiency, diode pumped solid state lasers constructions.

Due to multifunction capabilities, planar active waveguides became promising for applications in integrated optical networks. In order to commercialise these devices, further progress in active material technology and characterisation, channel waveguide technology and optimisation of diode side- and longitudinal-pump configurations is needed.

Acknowledgments

The authors would like to thank Mrs. K. Mazur and Dr. J. Sass for X-ray diffraction measurements. This work was supported by the Polish Committee for Scientific Research under grant PBZ-023-10.

References

1. *Optical Fibre Telecommunications*, Vol. II, edited by S.E. Miller and I.P. Kaminow, *Academic Press*, New York, 1988.
2. *Rare Earth Doped Fibre Lasers and Amplifiers*, edited by M.J.F. Digonnet, Marcel Dekker, Inc. New York-Basel-HongKong, 1993.
3. W.W. Kruhler, R.D. Plattner, W. Fabian, P. Mockel, and J.G. Grabmaier, "Laser oscillation of $Nd_{0.14}Y_{0.86}P_5O_{14}$ layers epitaxially grown on $Gd_{0.33}Y_{0.67}P_5O_{14}$ substrates," *Optics Comm.* **20**, 354–355 (1977).
4. E.D. Jungbluth, "Optical waveguides advance to meet fibreoptic demands," *Laser Focus World*, April, 99–104 (1994).
5. Ch. Wyon and B. Ferrand, "Laser guides d'ondes planaires compacts," *Ann. Chim. Fr.* **20**, 273–278 (1995).
6. E. Snoeks, *Optical Doping of Silica by Erbium Ion Implantation*, Ph.D. Thesis Utrecht University, 1995.
7. J.R. Bonar, J.A. Bebbington, J.S. Aitchison, G.D. Maxwell, and B.J. Ainslie, "Low threshold Nd-doped silica planar waveguide laser," *Electron. Lett.* **30**, 229–230 (1994).
8. J.R. Bonar, J.A. Bebbington, J.S. Aitchison, G.D. Maxwell, and B.J. Ainslie, "Aerosol doped Nd-planar silica waveguide laser," *Electron. Lett.* **31**, 99–100 (1995).
9. M.C. Farries, P.R. Morkel, R.L. Laming, T.A. Birks, D.N. Payne, and E.J. Tarbox, "Operation of erbium-doped fibre amplifiers and lasers pumped with frequency-doubled Nd:YAG lasers," *J. Lightwave Techn.* **7**, 1473–1477 (1989).
10. Y. Ohishi, T. Kanamori, T. Nishi, S. Takahashi, and E. Snitzer, "Gain characteristics of Pr^{3+}-Yb^{3+} codoped fluoride fibre for 1.3 μm amplification," *IEEE Trans. Phot. Tech. Lett.* **3**, 990–992 (1991).
11. N. Sugimoto, Y. Ohishi, Y. Katoh, A. Tate, M. Shimokozano, and S. Sudo, "A ytterbium- and neodymium-co-doped yttrium aluminum garnet-buried channel waveguide laser pumped at 0.81 μm," *Appl. Phys. Lett.* **67**, 582–584 (1995).
12. G. Winzer, L. Vite, W. Kruhler, R. Plattner, P. Mockel, and H. Pink, "Miniature neodymium lasers (MNL) as possible transmitters for fibre-optic communication systems," Part 1. Stoichiometric materials, *Siemens Forsch.- u. Entwickl.-Ber.* Bd. **5**, 287–295 (1976).
13. J. Nakano, K. Kubodera, S. Miyazawa, S. Kondo, and H. Koizumi, "$LiBi_xNd_{1-x}P_4O_{12}$ waveguide laser layer epitaxially grown on $LiNdP_4O_{12}$ substrate," *J. Appl. Phys.* **50**, 6546–6548 (1979).
14. F. Lutz, D. Ruppel, and M. Leiss, "Epitaxial layers of the laser material $Nd(Ga,Cr)_3(BO_3)_4$," *J. Crystal Growth* **48**, 41–44 (1980).
15. F. Lutz, M. Leiss, and J. Muller, "Epitaxy of $NdAl_3(BO_3)_4$ for thin film miniature lasers," *J. Cryst. Growth* **47**, 130-132 (1979).
16. P.K. Tien, "Light waves in thin films and integrated optics," *Appl. Opt.* **10**, 2395-2413 (1971).
17. H. Kogelnik and V. Ramaswamy, "Scaling rules for thin film optical waveguides," *Appl. Optics* **13**, 1857–1862 (1974).
18. P. Mockel, R. Plattner, W. Kruhler, A. Reichelt, and J. Grabmaier, "Miniature neodymium lasers (MNL) as possible transmitters for fibre-optic communication systems," Part 2. YAG:Nd^{3+} waveguide lasers," *Siemens Forsch.- u. Entwickl.-Ber.* Bd. **5**, 296–302 (1976).
19. D. Pelenc, B. Chambaz, I. Chartier, B. Ferrand, C. Wyon, D.P. Shepherd, D.C. Hanna, A.C. Large, and A.C. Tropper, "High slope efficiency and low threshold in a diode pumped epitaxially grown Yb:YAG waveguide laser," *Optics Comm.* **115**, 491–497 (1995).
20. D. Pelenc, *Elaboration par epitaxie en phase liquide et caracterisation de couches monocristallines de YAG dope, realisation de laser guides d'onde neodyme et ytterbium a faibles seuils*, Ph.D. Thesis Universite J. Fourieur, Grenoble 1993. (in French).
21. L. Zhang, P.D. Towsend, P.J. Chandler, and A.J. Silversmith, "Upoconversion in ion implanted Er:YAG waveguide," *Elect. Letters* **30**, 1063–1064 (1994).
22. S.J. Field, D.C. Hanna, A.C. Large, D.P. Shepherd, A.C. Tropper, P.J. Chandler, P.D. Towsend and L. Zhang, "Low treshold ion-implanted Nd:YAG waveguide laser," *Electron Lett.* **27**, 2375–2376 (1991).
23. D.C. Hanna, J.K. Jones, A.C. Large, D.P. Shepherd, A.C. Tropper, P.J. Chandler, M.J. Rodman, P.D. Towsend, and L. Zhang, "Quasi-three level 1.03-μm laser operation of a planar ion-implanted Yb:YAG waveguide," *Optics Comm.* **99**, 211–215 (1993).
24. J.E. Roman, P. Camy, M. Hempstead, W.S. Brocklesby, S. Nouch, A. Beguin, C. Lerminiaux, and J.S. Wilkinson, "Ion-exchanged Er/Yb waveguide laser at 1.5 μm pumped by laser diode," *Electron. Lett.* **31**, 1345–1346 (1995).
25. J.P. Van der Ziel, W.A. Bonner, L. Kopf, S. Singh, and L.G. Van Uitert, "Coherent emission from Ho^{3+} ions in epitaxially grown thin aluminum garnet films," *Phys. Lett.* **22**, 105–106 (1972).
26. J.P. Van der Ziel, W.A. Bonner, L. Kopf, S. Singh, and L.G. Van Uitert, "Laser oscillation from Ho^{3+} and Nd^{3+} ions in epitaxially grown thin aluminum garnet films," *Appl. Phys. Lett.* **22**, 656–657 (1973).
27. W.A. Bonner, "Epitaxial growth of garnets for thin film lasers," *J. Electron. Mat.* **3**, 193–208 (1974).
28. D.P. Shepherd, A.C. Large, T.J. Warburton, A.C. Tropper, D.C. Hanna, C. Borel, A. Remeix, Ph. Thony, B. Ferrand, S. Guy, B. Jacquier, and M.F. Joubert, "Epitaxial Yb:YAG

waveguide lasers at 2 μm and upconversion fluorescence in the blue and UV region," post-deadline paper presented at *European CLEO*, Amsterdam CPD 1.8., 1994.

29. P. Lacovara, H.K. Choi, C.A. Wang, R.L. Aggarwal, and T.Y. Fan, "Room-temperature diode-pumped Yb:YAG laser," *Optics Lett.* **16**, 1089–1091 (1991).
30. M. Shimokozono, N. Sugimoto, A. Tate, Y. Katoh, M. Tanno, S. Fukuda, and T. Ryuoh, "Room-temperature operation of an Yb-doped $Gd_3Ga_5O_{12}$ buried channel waveguide laser at 1.025 μm wavelength," *Appl. Phys. Lett.* **68**, 2177–2179 (1996).
31. J.E. Davies, E.A.D. White and J.D.C. Wood, "A study of parameters to optimise the design of LPE dipping apparatus," *J. Cryst. Growth* **27**, 227–240 (1974).
32. S.L. Blank and J.W. Nielsen, "The growth of magnetic garnet by liquid phase epitaxy," *J. Cryst. Growth* **17**, 302–311 (1972).
33. J. Sarnecki, M. Malinowski, J. Skwarcz, R. Jabłoński, K. Mazur, D. Litwin and J. Sass, "Liquid phase epitaxial growth and characterisation of Nd:YAG/YAG structures for thin film lasers," Proc. *SPIE* **4237**, 60–63 (2000).
34. R. Jabłoński, J. Sarnecki, K. Mazur, J. Sass, and J. Skwarcz, "ESR and X-ray diffraction measurements of Nd substituted yttrium aluminum garnet films," *J. Alloys & Comp.* **300/301**, 316–321 (2000).

